Investigation of atmospheric insect wing-beat frequencies and iridescence features using a multispectral kHz remote detection system

Gebru, Alem; Rohwer, Erich; Neethling, Pieter; Brydegaard, Mikkel

Published in:
Journal of Applied Remote Sensing

DOI:
10.1117/1.JRS.8.083503

2014

Journal of
Applied Remote Sensing

RemoteSensing.SPIEDigitalLibrary.org

Investigation of atmospheric insect wing-beat frequencies and iridescence features using a multispectral kHz remote detection system

Alem Gebru
Erich Rohwer
Pieter Neethling
Mikkel Brydegaard

SPIE.

Investigation of atmospheric insect wing-beat frequencies and iridescence features using a multispectral kHz remote detection system

Alem Gebru,[a,*] Erich Rohwer,[a] Pieter Neethling,[a] and Mikkel Brydegaard[a,b,c,d]

[a]Stellenbosch University, Laser Research Institute, Department of Physics, Private Bag X1, Matieland 7602, Stellenbosch, South Africa
[b]Lund University, Center for Animal Movement, Department of Biology, Sölvegatan 37, 223 62 Lund, Sweden
[c]Lund Laser Centre, Department of Physics, Sölvegatan 14, 223 62 Lund, Sweden
[d]Hyspex, Norsk Elektro Optikk, Solheimsveien 62A, 1473 Lørenskog, Norway

Abstract. Quantitative investigation of insect activity in their natural habitat is a challenging task for entomologists. It is difficult to address questions such as flight direction, predation strength, and overall activities using the current techniques such as traps and sweep nets. A multispectral kHz remote detection system using sunlight as an illumination source is presented. We explore the possibilities of remote optical classification of insects based on their wing-beat frequencies and iridescence features. It is shown that the wing-beat frequency of the fast insect events can be resolved by implementing high-sampling frequency. The iridescence features generated from the change of color in two channels (visible and near-infrared) during wing-beat cycle are presented. We show that the shape of the wing-beat trajectory is different for different insects. The flight direction of an atmospheric insect is also determined using a silicon quadrant detector. [DOI: 10.1117/1.JRS.8.083503]

Keywords: stand-off detection; remote dark-field detection; iridescence; optical cross-section; wing-beat frequency; quadrant detection; multiband scattering.

Paper 14560P received Sep. 19, 2014; accepted for publication Nov. 21, 2014; published online Dec. 18, 2014.

1 Introduction

Insects are the natural service providers of the ecosystem. They comprise approximately 80% of the animal population on earth.[1] They are pollinators, garbage collectors, and natural fertilizer producers. Insects are responsible for pollinating about 80% of flowering plants, e.g., bees.[2,3] They are excellent biomarkers of flowing water purity, pesticide abuse, or climatic change indicators.[4] Generally, insects play a crucial role in attaining the natural balance of the earth. On the other hand, insects can have a negative impact on agricultural productivity[5] and disperse forestry pests.[6,7] They can also transfer disease to livestock and humans.[8] Various species of mosquitoes can transfer diseases to human beings.[9] The study of insects has so far mainly been dependent on manual counting and analysis using, e.g., light traps, flight intercepts traps, pitfall traps, water pan trap, beating trays, and sweep nets.[10–15] Such methods have been used for many years, and have made significant contributions to the field of ecological entomology. However, it remains challenging to investigate fast interaction mechanisms or a vast number of insects using the conventional techniques *in situ*. To address those issues, it is important to implement more efficient and accurate insect-monitoring techniques. This could give a detailed understanding of insect activity, and it can help to get a better picture of the environment.

*Address all correspondence to: Alem Gebru, E-mail: gebru@sun.ac.za

0091-3286/2014/$25.00

Wide ranges of remote sensing techniques have been used for environmental monitoring purposes. Insect monitoring using fluorescence LIDAR (Light Detection and Ranging) technique was demonstrated by Brydegaard et al.[16] in Lund University. This feasibility study confirmed that the damselflies (*Calopteryx splendens and Calopteryx virgo*) exhibit reflectance and fluorescence properties, which are correlated with structural colors. Fluorescence LIDAR measurement was also performed by the same group.[17] The potential of LIDAR as a remote sensing tool to capture the activity of labeled damselfly species and genders was highlighted. This shows that the insect-monitoring techniques using fluorescence LIDAR can be used for other insect species such as mosquitoes, bees, and dragonflies. Some of the pioneering works that have been done in the area of elastic LIDAR by the Shaws group in Montana State University are the study of honeybees for sniffing land mines. Some of the techniques are scanning and polarization LIDAR measurements of bees,[18,19] optical detection of bees from their wing-beat frequency,[20] and range-resolved optical measurement of bees.[21] In general, the implementation of an optical remote sensing tool can provide reliable information to study activity and abundance of insects. Such techniques have the potential to remotely determine species, sex, and predation strength.[22] In the field of optical remote sensing of the atmospheric fauna, remote classification of nocturnal birds and the investigation of mid-infrared (MIR) iridescence features of plumage have also been done.[23,24] Such investigation demands expensive cooled detectors. The proposed setup provides complimentary data compared with existing techniques such as resolving fast wing-beat frequency and their higher harmonics. It enables the retrieval of important information such as flight direction and fast insect-insect interaction *in situ*. It is also inexpensive compared with entomological LIDARs or radars of comparable efficiency.

2 Equipment and Method

2.1 *Dark-Field Spectroscopy*

Remote dark-field spectroscopy was employed to investigate wing-beat frequencies and iridescence features of atmospheric insects *in situ*. We have used a Newtonian telescope (focal length = 1200 mm) coupled with silicon (Si) and Indium Gallium Arsenide (InGaAs) detectors and a CCD spectrometer to collect the backscattered signal from insect events crossing the field-of-view (FOV) (see Fig. 1). A cylindrical dark termination cavity was used to attain a

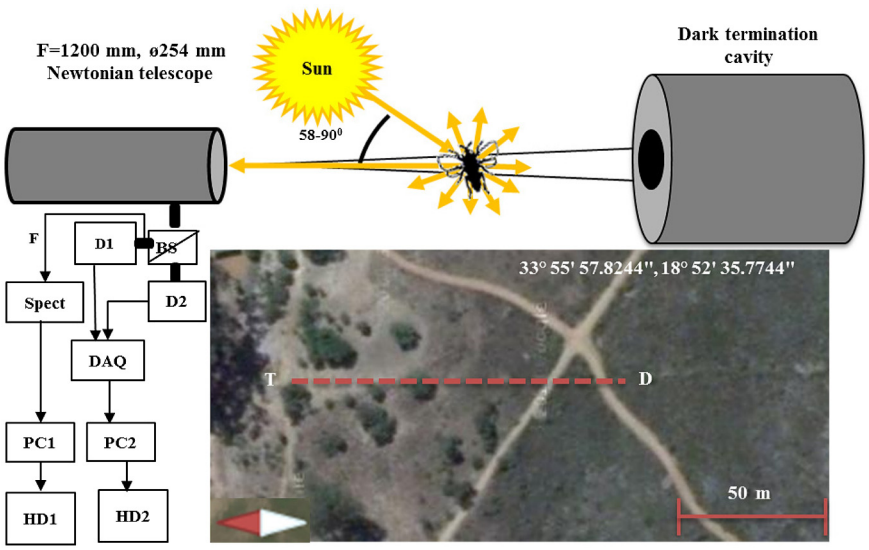

Fig. 1 Experimental setup. D1: detector 1 [silicon (Si) quadrant in part I and spectrometer in part II]; D2: Si/InGaAs sensors; F: fiber patch cable; Spect: spectrometer; DAQ: sampling device; BS: beam splitter; T: telescope; D: dark termination; PC1 and PC2: laptops for data collection; HD1 and HD2: data storing external hard drive. The distance between the telescope and dark termination is 200 m southwards, Jan Marias nature reserve, Stellenbosch, South Africa.

very low background signal.[22] The probe volume is the space between the receiving telescope aperture (T) and FOV at the dark termination (D). The air volume between T and D is the interrogated atmosphere, which we have monitored during a measurement. The object plane at termination for the quadrant and dual-band detectors is ø 60 cm, and the total air volume monitored is 92 m^3. The overall aim of this experiment is to be able to collect backscattered light from any event crossing the FOV. In the context of this work, an improved signal-to-background ratio can be achieved by keeping the termination box very dark or designing the termination box in such a way that it absorbs all incoming light. Ideally, the background signal is minimal, but there will still be scattering from the atmosphere itself and Rayleigh scattering even from pure air.

The concept of dark-field spectroscopy is more popular in microscopy, where dark field and fluorescence experiments provide better image contrast capabilities.[25–28] This is due to the fact that the signal rises from 0% rather than decreases from 100%, which is the case in, e.g., transmission measurements.

2.2 *Detector Setup and Spectral Band*

The experimental setup uses three detectors to cover the three bands: visible (VIS, 0.32 to 0.68 μm), near-infrared (NIR, 0.66 to 1 μm), and shortwave IR (SWIR, 1 to 2.4 μm). One detector is a Si photodiode, while the other two are Si photodiode and InGaAs photodiode, integrated into a layered package. This triple-band passive remote sensing tool is intended to determine wing-beat frequency, absolute optical cross-section (OCS) and iridescence features. The incoming light is gathered by the telescope and goes to the beam splitter (see Fig. 2). The beam splitter is a cold mirror, which is designed to reflect VIS light to the Si detector and transmit IR light to the Si/InGaAs detector. The beam walk displacement of the transmitted light was deviated by 1.6 mm from the optical axis due to the refraction in the cold mirror. To compensate for this, the dual-band detector was shifted by 1.6 mm using an external adaptor (off-set).

The resolution of the detectors covering the above bands is determined by the full-width half-maximum (FWHM) of individual bands. This crude spectral discrimination offers three bands with bandwidths from 0.3 to 1 μm FWHM (0.4 μm for the VIS, 0.3 μm for the NIR, and 1 μm for the SWIR) (see Fig. 4). Detector 1 is an Si quadrant detector which is sensitive in the VIS range, and Detector 2 is sensitive in the NIR and SWIR ranges. The second setup was designed to detect the spectral signature of insects using a spectrometer (Ocean Optics) and the wing-beat frequency using a Si/InGaAs detector. The Si quadrant was replaced by the spectrometer for the second part of the experiment. Some known insects such as dragonflies, damselflies, carotenoid beetles, and carpenter bees were released during the experiment into the FOV. The release timestamp was recorded in a logbook for latter lookup in the data stream. The second setup enables the retrieval of spectral information, wing-beat frequency, and OCS of insects concurrently.

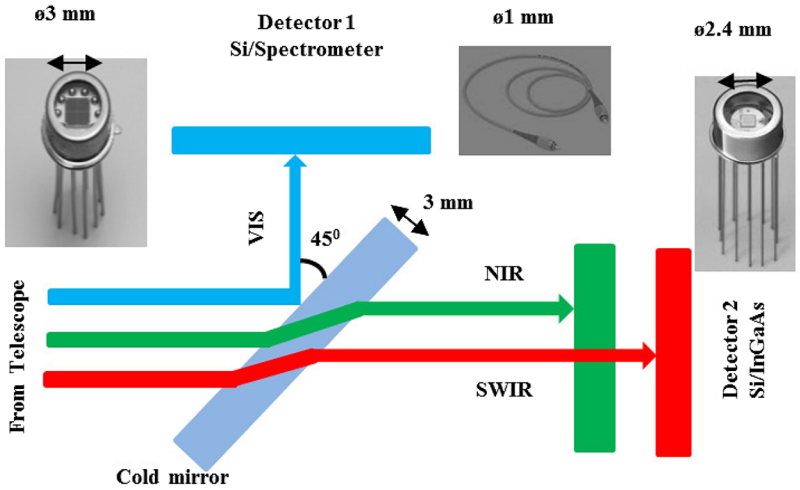

Fig. 2 Schematic plot of detector alignment for the first and second parts of the experiment.

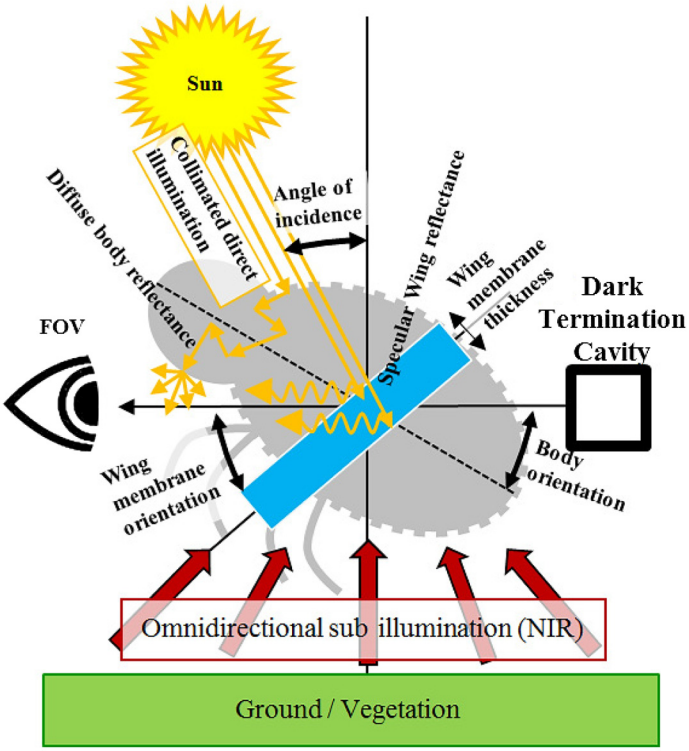

Fig. 3 Insect scattering processes. The passive remote sensing involves three scattering processes: melanin absorption in the visible (VIS), vegetation subillumination in the near-infrared (NIR), and thin-film iridescence (interfering waves).

The whole system described in Fig. 2 enables us to monitor VIS scattering, vegetation subillumination, melanization, and iridescence features simultaneously (see Fig. 3). The Si quadrant detector monitoring the VIS scattering provides information about the insect's flight direction and size. The NIR detector gives information about the subillumination of insects by upwelling radiation from vegetation, which helps to investigate the iridescence features of the insect by

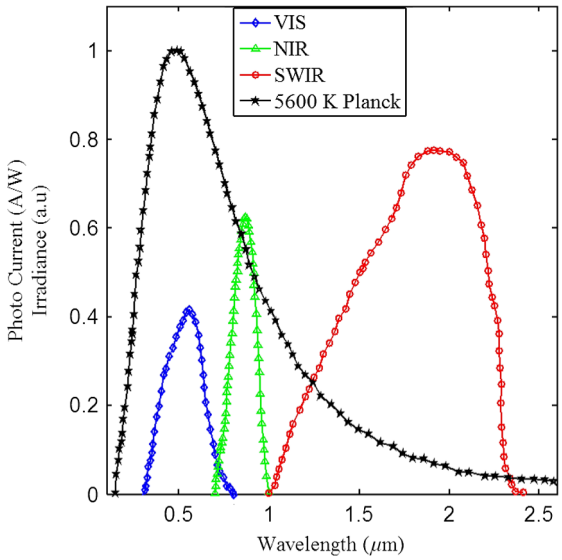

Fig. 4 Plot of sensitivity versus wavelength for the three detectors (data from supplier). VIS-Si (D1-Quadrant detector): VIS scattering, NIR-Si (D2): vegetation subillumination, and SWIR-InGaAs (D2): thin-film iridescence.

comparing the NIR signal with the VIS signal. We have two different effective light sources in this case: collimated sun emission, which is a 5600-K Planck distribution and incident from above, and the vegetation, which is the solar spectrum times a step around 700 nm. Further, it is an omnidirectional source from below. The SWIR detector provides information about the thin film interference from the spectral fringes of the signal caused in the conditions of specular reflections, which can be seen as spikes in the time signal.

The triple-band detector covers the wavelength range from 0.32 to 2.4 μm (see Fig. 4). The main advantage of this system as compared with a spectrometer is its higher sampling frequency. The extent of resolving wing-beat modulation of fast insect events depends on the sampling frequency.[29,30] The sampling frequency we implemented was 20 kHz, which is fast enough to resolve harmonic overtones of insects with fast wing-beats such as mosquitoes.

3 Results

The experimental results presented here are from two sites in Stellenbosch, South Africa [Jan Marais Nature reserve (33° 55′ 57.8244″, 18° 52′ 35.7744″) and Stellenbosch University campus (33° 55′ 58.9404″, 18° 51′ 58.3194″)].

3.1 *Wing-Beat Frequency, Flight Direction, and Absolute Optical Cross-Section*

Two of the most important quantities that could be used to identify insects remotely are wing-beat frequency and absolute OCS. The absolute OCS is the size of the insect times the effective reflectance for the given band. The quantitative estimate comes from the calibration of the setup using white diffuse spheres. The calibration was performed by releasing different sized diffuse white spheres close to the dark termination in the FOV. This means that after subtraction of the detector dark current and static atmospheric contributions, the absolute OCS is calibrated by white diffuse spheres with known diameters and an assumed 100% Lambertian reflectance. For example, a certain insect event with wing-beat frequency of 143 Hz and an absolute OCS of approximately 20 mm^2 was detected (see Fig. 5).

The calculated absolute OCS can in some cases exceed the projected actual size due to specular reflections. In future, this could be improved by using polarimetric detection for retrieving the coherent and incoherent scatters separately. Because of the range-dependent sensitivity or form factor,[31] the absolute OCSs in this paper are only accurate close to the

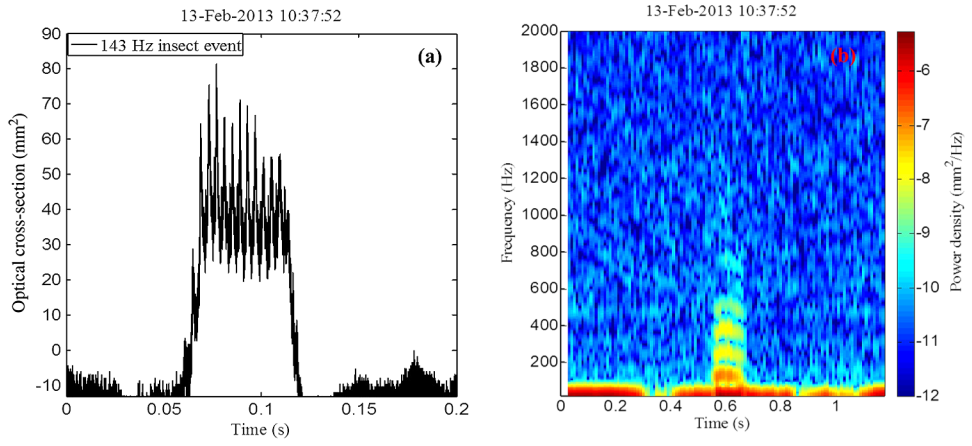

Fig. 5 (a) Wing-beat frequency and OCS (mm^2) of a certain insect event. (b) Spectrogram showing body size, fundamental frequency, and harmonic overtones of the same insect event. The DC level shows the body size. The fundamental frequency at 143 Hz and the higher order harmonic are shown.

object plane and the termination where the calibration and controlled releases were performed. The accuracy of absolute OCS using the proposed setup and range-resolved measurements, such as LIDAR, could be comparable for positions close to the object plane. However, limited range information can be extracted from the flank rise and fall times that can be associated with the event distance from the object plane using the proposed setup. In order to further improve the accuracy of absolute OCS, one has to look at the steepness of the rise/fall flanks of events, but this was not fully investigated in this study. An additional uncertainty when relating the projected absolute OCS to the actual body size is the flight direction and body orientation, which is also an issue in range-resolved LIDAR measurements. However, limited assessment of the orientation could be retrieved from the quadrant information and from the relative strength between odd and even harmonics.[32]

A pendulum was implemented to determine the flight direction of insects. The calibration was done by oscillating the pendulum sweeping through the FOV from East to West for about 10 to 20 s at the object plane. This process was repeated every 30 min throughout the measurement session to quantify the light power impinging on the FOV during the day. From this, we were able to suggest the orientation of the quadrant and this was then correlated with the flight direction (see Fig. 6).

The dynamics of prey and predator interaction is one of the important aspects of entomological ecology studies. This kind of investigation can give information about predators of a certain insect, which in turn leads to natural ways of improving conditions for predators in order to suppress pests or infectious insect species like mosquitoes. It may also help to understand seasonal dynamics and populations;[33,34] however, it should be noted that this experiment mainly focuses on the dynamics with millisecond resolution. In this work, we detected several chasing events. An example can be seen in Fig. 7. The time difference between the two consecutive insects is 0.5 s. A precise description of the interaction strength and the kinetics can be evaluated through a time-lag correlation of a large number of such events.[22] The body absolute OCS and wing-beat frequency of the first insect (left) are approximately 23 mm^2 and 100 Hz, respectively. For the second insect (right), the body absolute OCS and wing-beat frequency are approximately 96 mm^2 and 50 Hz, respectively. The absolute OCS (size) difference between the two insect events mentioned in Fig. 7 is 25%. This shows that a bigger (lower wing-beat frequency) was chasing a smaller (higher wing-beat frequency) insect. A number of insect events similar to this occurred during the field campaign, which leads us to believe that this is predation and not a simple coincidence.

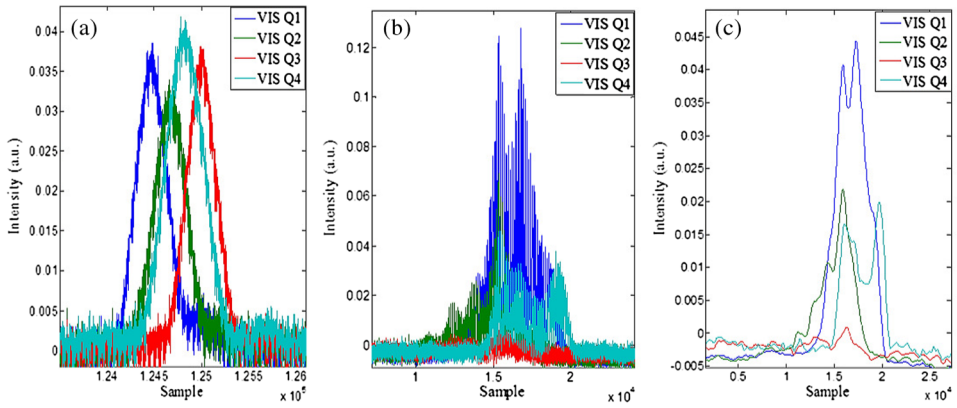

Fig. 6 (a) Signal recorded by the Si quadrants (Q1, Q2, Q3, and Q4) from pendulum oscillation (east to west). The time sequence of the signal shows that the pendulum first enters Q1 (east) and exists at Q3 (west). The quadrant orientation suggestion in this case is: Q1-East, Q2-Down, Q3-West, and Q4-Up relative to each other. (b) Signal from the insect event detected by the quadrant detector. (c) Smoothed wing-beat signal [the original signal in (b) is filtered by a zero-phase Gaussian with the width of the wing-beat periodicity], which helps to see the distribution of the signal from each quadrant of the insect event in (b). The insect enters Q2 → Q1 → Q4 sequentially, but it was not detected on Q3.

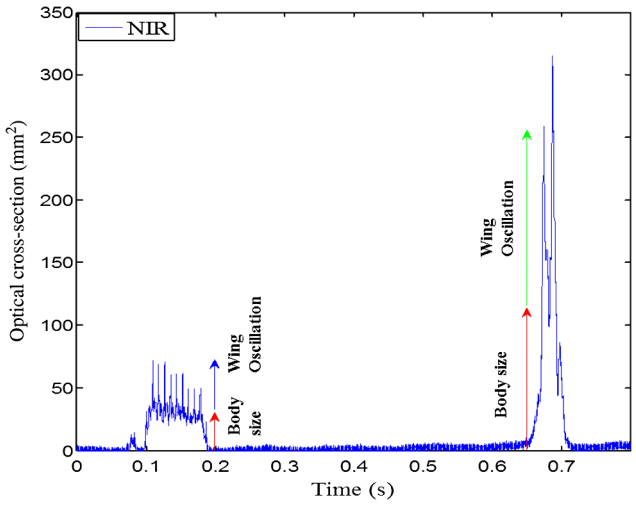

Fig. 7 Example of a chasing event likely due to predation. Red arrows: Body sizes of small (left) and big (right). Blue and green arrows: wing oscillation of the small and big insect, respectively. The time difference between the two insect events is 0.5 s.

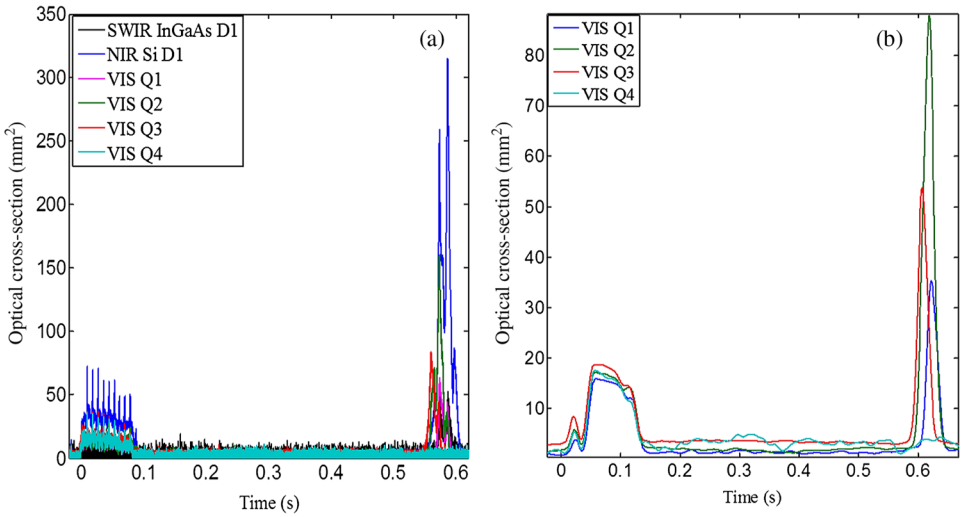

Fig. 8 (a) Triple-band signal of five insect events in the VIS, NIR, and SWIR. (b) Smoothed signal (Gaussian filtered) of the chasing event. This is a signal only from the quadrant detector, which shows the time sequence of the insect entering different segments of the detector. The smaller insect (left) enters Q3, Q2, and Q1 sequentially and the bigger insect (right) follows similar path after 0.5 s.

The chasing insect event in Fig. 7 was recorded in three bands (VIS Si-Quadrant, NIR Si, and SWIR InGaAs) (see Fig. 8). From this, one can get wing-beat frequency and directional information of the insect simultaneously. In reality, it is difficult to know whether the two events in Fig. 7 happen at the same range or are separated along the monitored path, since we cannot retrieve range information in this experiment. However, it could be possible to confirm this situation if we coupled the temporal dynamics with the directional information from the quadrant. Figure 8(b) shows that the smaller insect (left) enters the FOV from West first before the arrival of the larger insect (right) and they follow each other. The sequence is the same for both insects except that the smaller insect was detected flying upward, but not the bigger insect. This means that it is more likely that the larger insect was following the smaller one at the same location in the FOV. Therefore, we could say that it is possible to confirm a chasing event by correlating the

millisecond time dynamics with directional information, even though we cannot retrieve range information and verify the spatial co-occurrence using the proposed setup.

3.2 *Iridescence Features*

Iridescence refers to a change of spectral signature with a change of angle of detection or illumination of a certain object. This concept has been used to study the structural color of biological samples, e.g., the iridescence in the neck feathers of pigeons shows that cyan feathers change color to magenta at large viewing-illumination angles.[35,36] Many investigations have also been done to investigate the nature of the structural color of insects, which show stable patterns in different insect species.[37–41] In this work, we have remotely investigated the iridescence features of insects. This is a situation where an object changes its spectral signature when illuminated by different colors (see Fig. 9).

We have used a Si quadrant and a two-color detector (Si/InGaAs). The Si quadrant detector monitors the VIS range. The Si part within the two-color detector monitors the NIR, and the InGaAs part monitors the SWIR. All backscattered light was collected simultaneously from any insect event crossing the FOV. We have used only two-bands for this investigation. We did this in order to study the difference in the shape of the waveform in the VIS and NIR [see Fig. 9(a)]. The temporal signal of a certain insect in the VIS and NIR is found to be different as expected [see Fig. 9(b)]. The ratio of NIR and VIS is not constant, since there is a difference in the temporal signal. This difference in waveform of the temporal signal could be due to wing melanization[42] on the slow part of the wing-beat in the VIS and vegetation subillumination in the NIR. Melanin is the most common chromophore[43] of all insects, which is responsible for dull black and brownish colors. The membrane thickness should manifest as a spectral modulation in the temporal signal at instances of the specular reflection. This was not fully investigated in this study. The trajectory in a VIS-NIR color space of the insect event in Fig. 9 has shown specific features (see Fig. 10). These features will be discussed more in the next section.

Investigation of the trajectory in a VIS-NIR-SWIR color space is one useful aspects of insect studies. It should be noted that this is an extension of the well-known Red-Green-Blue (RGB) color space concept. This is directly related to the waveform of a wing-beat cycle. Each temporal waveform has a different amplitude, harmonic content, and phase.[23] These quantities can be exploited to generate trajectories in a two-dimensional (2-D) color plane (see Fig. 10). The trajectories for different insect species are different because of differences in terms of position, phase, modulation size, and direction of the temporal waveform. This seems to be species specific, but it requires a controlled experiment with known insects to verify this. A comparison of

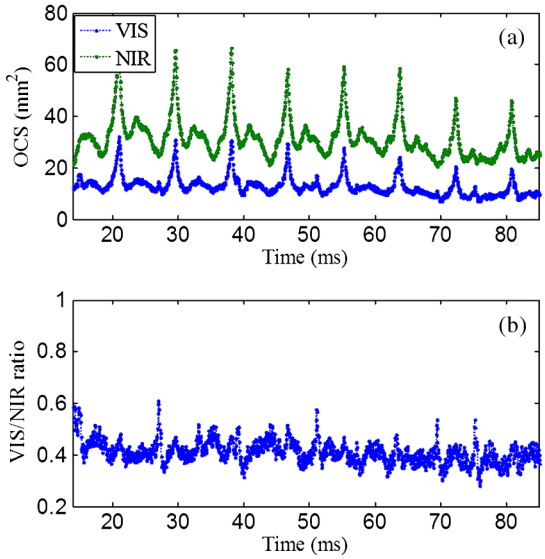

Fig. 9 Iridescent properties: (a) spectral difference in the VIS and NIR ranges. (b) Ratio of VIS and NIR. Note the entirely different waveform.

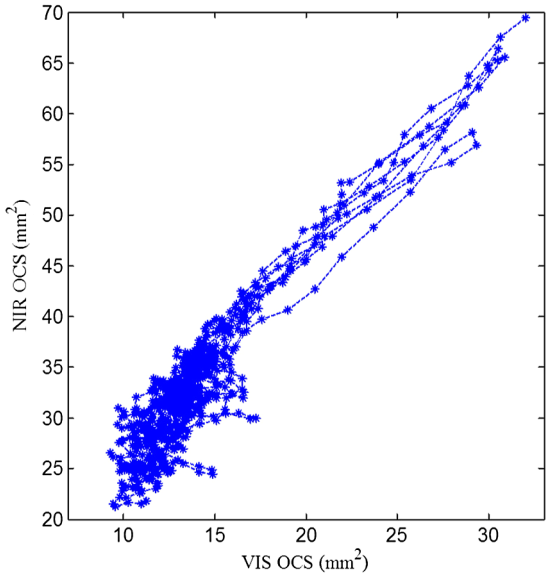

Fig. 10 Trajectory in color plane during five wing-beat cycles. This representation could help to distinguish insect species.

wing-beat trajectories among different insect species is given in the next section. As noted, the trajectory in color space is one way of visualizing the difference in the temporal waveform of the insect and this can be used for remote identification of insect species. To illustrate this, we can consider the chasing event[22] (see Fig. 11).

The two insects have different sizes and wing-beat frequencies (see Fig. 11). By looking at this specific event, one can guess that they are different species. However, it is interesting to see if there is a difference between the trajectories in color space of both insects. The trajectory of the smaller insect has a smaller modulation size than the bigger insects and this could be due to their size differences. The reason why the shape of the trajectory is different could be due to a variation of wing melanization in the VIS and vegetation subillumination in the NIR. We have made a comparison of three different insects and analyzed the differences in order to enrich and support the aforementioned concept. It is found that this analysis is also in agreement with the above discussion. This result shows that the trajectory in the 2-D color plane is different for the three

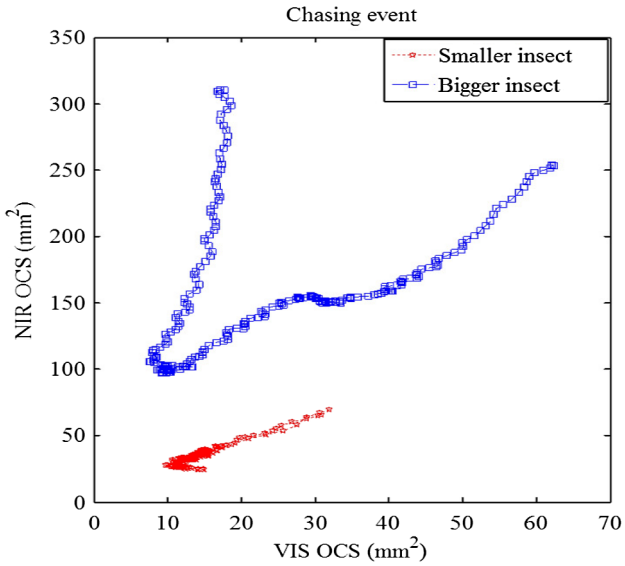

Fig. 11 Trajectory in color space for chasing insect event. NIR OCS: near-infrared optical cross-section and VIS OCS: visible optical cross-section.

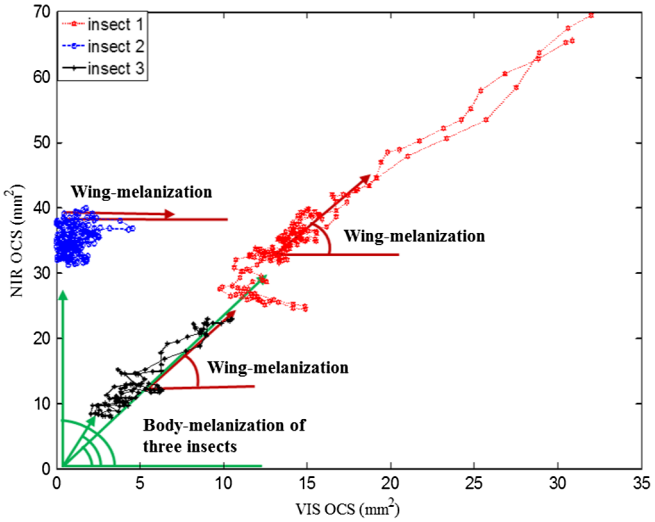

Fig. 12 Trajectory in two-dimensional (2-D) VIS-NIR color plane for three insects with different sizes and wing-beat frequencies. NIR OCS: near-infrared optical cross-section and VIS OCS: visible optical cross-section. Wing melanization is related to the slope of oscillation and body melanization is related to the off-set. Melanin is the most common chromophore of all insects, which is responsible for colors.

insect species (see Fig. 12). The slope of oscillation and off-set are related to the wing and body melanization, respectively. In this case, a large angle means more body or wing melanization of a certain insect. The assessment of the degree of melanization could improve species selectivity. This could also be reproducible for other similar insect species, and it could help to map insects based on their wing-beat trajectories. The result in Fig. 12 is inspired by laboratory work done in Ref. 23, which presented significantly different MIR signatures for a list of bird species. The trajectories for the six species showed significant differences.

3.3 *Insect Release*

The purpose of this experiment was to detect reflecting color marked insects concurrently using a spectrometer and a two-color detector. We have made known insect releases during this

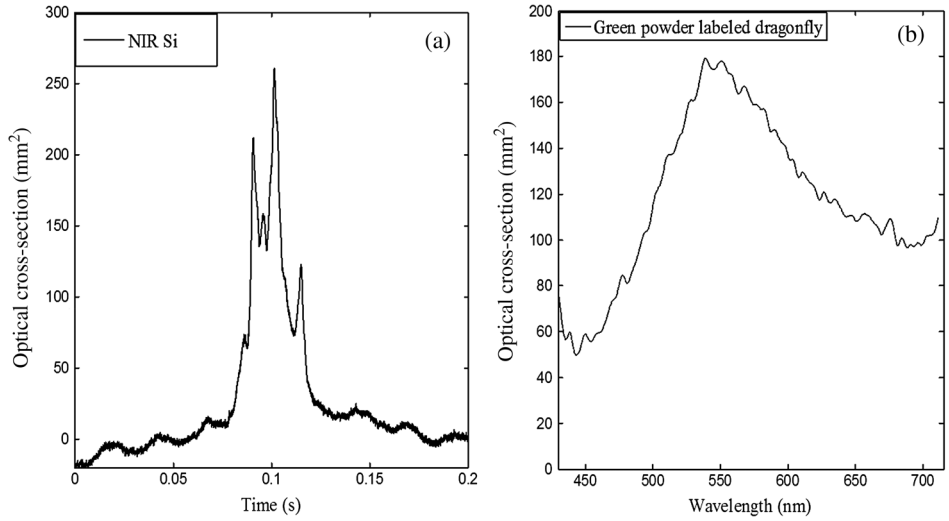

Fig. 13 Released green powder-labeled dragonfly: (a) wing-beat frequency of dragonfly using Si-NIR detector. (b) Spectral signatures of dragon fly using spectrometer.

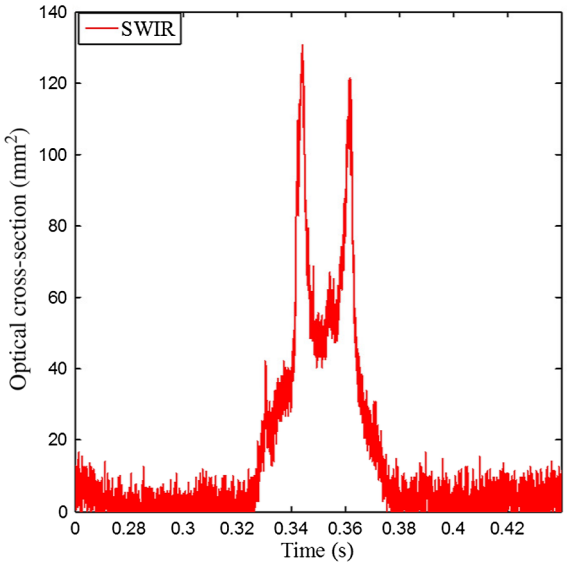

Fig. 14 Insect event detected by the SWIR detector. Wing-beat frequency and size of the insect are 66 Hz and 30 mm^2, respectively.

experiment to verify the capability of the technique. This setup enables us to retrieve spectral signature, wing-beat frequency, and absolute OCS information simultaneously (see Fig. 2). One of the released insects was a green powdered dragonfly and we detected the event with the spectrometer and Si (NIR) part of the two-color detector (Si/InGaAs) (see Fig. 13). Figures 13(a) and 13(b) show the backscattering signal from the dragonfly which contains wing-beat frequency information and the spectral signature, which has predominantly green features due to the powder, respectively. The wing-beat frequency is 71 Hz, which is in the expected range for a dragonfly. This was detected with the NIR detector. This event was not detected by the SWIR detector. The reason for this could be because the dragonfly hits the edge of the FOV, since the size of the Si (NIR) is slightly bigger than that of the InGaAs (SWIR). However, we can confirm that the SWIR detector works well and we have detected some insect events, e.g., 66 Hz insect (see Fig. 14). A few other insects (e.g., damselfly, carpenter bee, honey bee, and moths) were released during our experiment, but some of them did not enter the FOV and others produced relatively a weak backscattered signal. We found that there was a difference in signal strength among the different insect species. This could be due to insect size differences, flight headings, and detection range.

4 Discussion and Conclusion

We have developed and tested a multispectral kHz remote detection system, capable of resolving the wing-beat frequency of fast insect events. This technique enables us to get a rough estimation of the absolute OCS. It should be noted that the improvements can be made by considering the distance from the focus and the rise times. This technique can also be used to remotely investigate the iridescence features of insects. Simultaneous remote monitoring of insects on three bands is presented. It is shown that this technique can be used for species classification and to determine the flight direction of an atmospheric insect. The uncertainty of chasing events can also be minimized by correlating information from the quadrant and the two-color detector. We discussed the possibility of estimating wing-membrane thickness remotely using the current technique. Generally, this remote detection system has shown potential for future studies of insect activities and we can say that wing-beat frequency, absolute OCS, spectral signature, and iridescence features could provide a means to remotely identify insects. In the future, we plan to investigate this farther using the concepts of thin films[44–50] to estimate the membrane thickness of insect wings.

Acknowledgments

We want sincerely thank Anna Runemark, Maren Wellenreuther, Nanike Esterhuizen, and John Terblanche for helping out during the field campaigns. We want to thank the Physics Department, Stellenbosch University, Gerhard Louwrens, and Lawrence Ashworth for helping us build the dark termination box, pendulum, and some adaptors, and we are grateful for all assistance given by the staff. We want to thank Jan Marias Nature Reserve for allowing us to host the workshop and campaign.

References

1. R. Costanza et al., "The value of the world's ecosystem services and natural capital," *Nature* **387**(6630), 253–260 (1997).
2. R. Costanza, "Introduction—special section: Forum on valuation of ecosystem services—the value of ecosystem services," *Ecol. Econ.* **25**(1), 1–2 (1998).
3. R. Costanza et al., "The value of the world's ecosystem services and natural capital [Reprinted from Nature 387, 253 (1997)]," *Ecol. Econ.* **25**(1), 3–15 (1998).
4. R. Hickling et al., "A northward shift of range margins in British Odonata," *Global Change Biol.* **11**(3), 502–506 (2005).
5. C. M. Oliveira et al., "Crop losses and the economic impact of insect pests on Brazilian agriculture," *Crop Prot.* **56**, 50–54 (2014).
6. P. D. Coley and T. A. Kursar, "On tropical forests and their pests," *Science* **343**(6166), 35–36 (2014).
7. G. M. Lovett et al., "Forest ecosystem responses to exotic pests and pathogens in eastern North America," *Bioscience* **56**(5), 395–405 (2006).
8. P. Azambuja, E. S. Garcia, and N. A. Ratcliffe, "Gut microbiota and parasite transmission by insect vectors," *Trends Parasitol.* **21**(12), 568–572 (2005).
9. J. Wang et al., "*Anopheles gambiae* circumsporozoite protein-binding protein facilitates plasmodium infection of mosquito salivary glands," *J. Infect. Dis.* **208**(7), 1161–1174 (2013).
10. S. Broughton and J. Harrison, "Evaluation of monitoring methods for thrips and the effect of trap colour and semiochemicals on sticky trap capture of thrips (Thysanoptera) and beneficial insects (Syrphidae, Hemerobiidae) in deciduous fruit trees in Western Australia," *Crop Prot.* **42**, 156–163 (2012).
11. D. Broederbauer, A. Weber, and A. Diaz, "The design of trapping devices in pollination traps of the genus Arum (Araceae) is related to insect type," *Bot. J. Linn. Soc.* **172**(3), 385–397 (2013).
12. R. A. De Clerck-Floate, P. Saunders, and K. D. Floate, "Release and recapture of three insect species test the efficacy of trap method and air flow in insect containment," *Can. Entomol.* **144**(4), 609–616 (2012).
13. F. J. Dirrigl, Jr., "Effectiveness of pan trapping as a rapid bioinventory method of freshwater shoreline insects of subtropical Texas," *Southwest. Entomol.* **37**(2), 133–139 (2012).
14. B. A. Krimmel and I. S. Pearse, "Sticky plant traps insects to enhance indirect defence," *Ecol. Lett.* **16**(2), 219–224 (2013).
15. J. A. Tansey et al., "A novel trapping system for monitoring insect flight heights," *Can. Entomol.* **144**(4), 617–620 (2012).
16. M. Brydegaard et al., "Insect monitoring with fluorescence lidar techniques: feasibility study," *Appl. Opt.* **48**(30), 5668–5677 (2009).
17. Z. Guan et al., "Insect monitoring with fluorescence lidar techniques: field experiments," *Appl. Opt.* **49**(27), 5133–5142 (2010).
18. J. A. Shaw et al., "Polarization lidar measurements of honey bees in flight for locating land mines," *Opt. Express* **13**(15), 5853–5863 (2005).
19. E. S. Carlsten et al., "Field demonstration of a scanning lidar and detection algorithm for spatially mapping honeybees for biological detection of land mines," *Appl. Opt.* **50**(14), 2112–2123 (2011).

20. K. S. Repasky et al., "Optical detection of honeybees by use of wing-beat modulation of scattered laser light for locating explosives and land mines," *Appl. Opt.* **45**(8), 1839–1843 (2006).
21. D. S. Hoffman et al., "Range-resolved optical detection of honeybees by use of wing-beat modulation of scattered light for locating land mines," *Appl. Opt.* **46**(15), 3007–3012 (2007).
22. A. Runemark et al., "Rare events in remote dark-field spectroscopy: an ecological case study of insects," *IEEE J. Sel. Top. Quantum Electron.* **18**(5), 1573–1582 (2012).
23. M. Brydegaard et al., "On the exploitation of mid-infrared iridescence of plumage for remote classification of nocturnal migrating birds," *Appl. Spectrosc.* **67**(5), 477–490 (2013).
24. P. Lundin et al., "Remote nocturnal bird classification by spectroscopy in extended wavelength ranges," *Appl. Opt.* **50**(20), 3396–3411 (2011).
25. R. Leary et al., "Quantitative high-angle annular dark-field scanning transmission electron microscope (HAADF-STEM) tomography and high-resolution electron microscopy of unsupported intermetallic GaPd2 catalysts," *J. Phys. Chem. C* **116**(24), 13343–13352 (2012).
26. K. M. Mitsuishi, "Imaging properties of bright-field and annular-dark-field scanning confocal electron microscopy," *Ultramicroscopy* **111**(1), 20–26 (2010).
27. T. A. Nenasheva, "Automatic tracking of individual migrating cells using low-magnification dark-field microscopy," *J. Microsc.* **246**(1), 83–88 (2012).
28. G. S. Verebes et al., "Hyperspectral enhanced dark field microscopy for imaging blood cells," *J. Biophotonics* **6**(11–12), 960–967 (2013).
29. B. Wen et al., "Experimental verification of the generalized Nyquist stability criterion for balanced three-phase Ac systems in the presence of constant power loads" in *4th Annual IEEE Energy Conversion Congress and Exposition, ECCE 2012*, pp. 3926–3933 (2012).
30. R. Turner, S. Walton, and R. Duke, "A case study on the application of the Nyquist stability criterion as applied to interconnected loads and sources on grids," *IEEE Trans. Ind. Electron.* **60**(7), 2740–2749 (2013).
31. H. Kuze et al., "Field-of-view dependence of lidar signals by use of Newtonian and Cassegrainian telescopes," *Appl. Opt.* **37**(15), 3128–3132 (1998).
32. S. Torok, "Kiloherz electro-optics for remote sensing of insects," Lund Reports on Combustion Physics, LRCP-171, ISNR LUTFD2/TFC-171-SE, Vol. ISSN (2013).
33. B. Giffard et al., "Bid predation enhances tree seedling resistance to insect herbivores in contrasting forest habitats," *Oecologia* **168**(2), 415–424 (2012).
34. R. Rodriguez-Munoz, A. Bretman, and T. Tregenza, "Guarding males protect females from predation in a wild insect," *Curr. Biol.* **21**(20), 1716–1719 (2011).
35. H. Yin et al., "Iridescence in the neck feathers of domestic pigeons," *Phys. Rev. E* **74**(5), 051916 (2006).
36. K. J. McGraw, "Multiple UV reflectance peaks in the iridescent neck feathers of pigeons," *Naturwissenschaften* **91**(3), 125–129 (2004).
37. E. Lee, M. Aoyama, and S. Sugita, "Microstructure of the feather in Japanese Jungle Crows (*Corvus macrorhynchos*) with distinguishing gender differences," *Anat. Sci. Int.* **84**(3), 141–147 (2009).
38. S. M. Doucet et al., "Concordant evolution of plumage colour, feather microstructure and a melanocortin receptor gene between mainland and island populations of a fairy-wren," *Proc. R. Soc. B-Biol. Sci.* **271**(1549), 1663–1670 (2004).
39. I. Galvan, "Feather microstructure predicts size and colour intensity of a melanin-based plumage signal," *J. Avian Biol.* **42**(6), 473–479 (2011).
40. E. Lee et al., "Feather microstructure of the black-billed magpie (Pica pica sericea) and jungle crow (*Corvus macrorhynchos*)," *J. Vet. Med. Sci.* **72**(8), 1047–1050 (2010).
41. F. M. Lei et al., "The feather microstructure of Passerine sparrows in China," *J. Fur Ornithol.* **143**(2), 205–212 (2002).
42. H. Kan et al., "Molecular control of phenoloxidase-induced melanin synthesis in an insect," *J. Biol. Chem.* **283**(37), 25316–25323 (2008).
43. T. Seki et al., "Flies in the group Cyclorrhapha use (3s)-3-hydroxyretinal as a unique visual pigment chromophore," *Eur. J. Biochem.* **226**(2), 691–696 (1994).

44. Y. Lo, Y. Chung, and H. Lin, "Polarization scanning ellipsometry method for measuring effective ellipsometric parameters of isotropic and anisotropic thin films," *J. Lightwave Technol.* **31**(14), 2361–2369 (2013).
45. S. G. Choi et al., "Temperature-dependent optical properties of epitaxial CdO thin films determined by spectroscopic ellipsometry and Raman scattering," *J. Appl. Phys.* **113**(18), 183515 (2013).
46. W. Ogieglo et al., "n-Hexane induced swelling of thin PDMS films under non-equilibrium nanofiltration permeation conditions, resolved by spectroscopic ellipsometry," *J. Membr. Sci.* **437**, 313–323 (2013).
47. E. R. Shaaban, "Optical constants and fitted transmittance spectra of varies thickness of polycrystalline ZnSe thin films in terms of spectroscopic ellipsometry," *J. Alloys Compd.* **563**, 274–279 (2013).
48. A. Shan et al., "High-speed imaging/mapping spectroscopic ellipsometry for in-line analysis of roll-to-roll thin-film photovoltaics," *IEEE J. Photovoltaics* **4**(1), 355–361 (2014).
49. H. A. Al-Khanbashi et al., "Spectroscopic ellipsometry of Zn1-xCuxO thin films based on a modified sol gel dip-coating technique," *Spectrochim. Acta, Part A* **118**, 800–805 (2014).
50. S. Kinoshita, S. Yoshioka, and J. Miyazaki, "Physics of structural colors," *Rep. Prog. Phys.* **71**(7), 076401 (2008).

Alem Gebru received his bachelor's degree in physics, Mekelle University in 2006. He was employed by Mekelle University and worked in different positions (graduate assistant and assistant lecturer) until 2008. He received a master's degree in physics in 2010 from Lund University, Sweden. He is currently working on his PhD project in Stellenbosch University and has strong collaboration with Lund University, Sweden. His research focus is on laser radar and optical remotes sensing of atmospheric fauna.

Erich Rohwer received his PhD degree in physics from Stellenbosch University in 1992. He joined the Stellenbosch University Physics Department in 1989 and was appointed as a professor in physics in 2007. He is a member of the Laser Research Institute in the department. He has a broad interest in laser spectroscopy and laser applications: CO_2 laser development, vacuum ultraviolet laser spectroscopy, surface second-harmonic generation at surfaces using femtosecond lasers, and spatial light modulation applications.

Pieter Neethling received his PhD degree in laser physics from Stellenbosch University in 2008. He has published numerous laser spectroscopy-related papers. Currently, he is employed as a lecturer at Stellenbosch University. In recent years, his research focus has shifted from basic research toward more applied interdisciplinary research, with special emphasis on questions within the biological sciences. His interests include nonlinear spectroscopy, Raman spectroscopy, THz spectroscopy, and remote sensing techniques.

Mikkel Brydegaard received his PhD degree in atomic physics from Lund University 2012. He has developed applied optical spectroscopy, biophotonics, chemometrics, and laser radar for almost one decade. He has a passion for realistic instrumentation and optical science in Africa and South America, where he has been organizing training activities for several years. In recent years, his research is focusing on laser radar and optical remote sensing of the atmospheric fauna.